J. Phys. Chem. 1990, 94, 222-227

Supersonic Jet Studies of Fluorene Clustered with Water, Ammonia, and Piperidine

H. S. Im, V. H. Grassian, and E. R. Bernstein*

Department of Chemistry, Colorado State University, Fort Collins, Colorado 80523

(Received: May 30, 1989)

Mass-resolved excitation spectroscopy and dispersed emission spectroscopy are employed to study van der Waals (vdW) clusters of jet-cooled fluorene with ammonia, water, and piperidine. For fluorene$(H_2O)_1$ and fluorene$(NH_3)_1$ clusters, cluster geometries and binding energies can be suggested based on the experimental results and Lennard-Jones (LG) potential (6-12-1) energy calculations. As the number of solvent molecules in the cluster is increased, spectra of the clusters become more complex and broad probably due to the many possible stable configurations for these vdW clusters. Although the pK_a for fluorene in its first excited singlet state (Förster cycle calculations) is quite acidic (−8.6), and solvent molecules can coordinate to the aliphatic hydrogens of the fluorene molecule in at least some cluster configurations, no direct evidence is found for the occurrence of proton transfer in S_1 in these systems.

Introduction

The acidities of aromatic hydrocarbons in their first excited singlet states can be predicted by using Förster cycle calculations.[1] Based on this calculation, the pK_a of fluorene in the first excited single state S_1 has been estimated to be −8.6, whereas it is measured to be 20.5 in the ground state, S_0.[2] Because of this large electronic redistribution upon electronic excitation in fluorene, very different acid–base properties, dipole moment, and solvent organization can be expected for the ground and first excited singlet states. The aliphatic protons in fluorene might then become labile in S_1, making fluorene a good candidate for the study of intermolecular proton-transfer dynamics.

Recent gas-phase studies have demonstrated that solvent-mediated intermolecular proton-transfer reactions can be investigated by using supersonic molecular jet spectroscopy. These reactions are confirmed by observing broad and red-shifted fluorescence originating from the S_1 state of the anion formed from the proton transfer. The minimum number of solvent molecules N_c required for proton transfer has also been determined.

In the proton-transfer reaction of α-naphthol with ammonia, N_c has been determined to be 4.[3-5] In a related set of experiments on ions, Jouvet has proposed that proton transfer may occur in phenol/ammonia complexes when the number of ammonia molecules exceeds 4.[6] Nimlos et al. have determined that the proton transfer occurs in 2-hydroxypyridine/ammonia clusters for $n \geq 3$.[7]

These studies demonstrate that in vdW clusters a number of solvent molecules must be present to induce proton transfer: some minimum degree of solvation of the proton and/or anion by solvent molecules is necessary for proton transfer to occur.

Supersonic jet techniques are typically employed for generating and studying the various requisite vdW clusters.[8] vdW clusters of fluorene with water, ammonia, and piperidine are produced in the supersonic jet expansion and are then identified and investigated by mass-resolved excitation spectroscopy (time-of-flight mass spectroscopy (TOFMS)) and dispersed emission (DE) spectroscopy.

In this report, we present and analyze mass-resolved excitation data, DE data, and the results of potential energy calculations for fluorene complexed with water, ammonia, and piperidine. The calculations help in the determination of the cluster configuration, binding energies, and the expected cluster spectroscopic shifts. We have found them quite helpful in the overall determination of the behavior of these clusters.[9] The possibility of an intermolecular proton-transfer reaction in fluorene complexes will be discussed on the basis of experimental observations and calculations.

TABLE I: Atomic Partial Charges for the Fluorene Molecule

atoms[a,b]	partial charges	atoms[a,b]	partial charges
C1	−0.0407	C13	−0.0879
C2	−0.0407	H14	0.1338
C3	−0.0773	H15	0.1338
C4	−0.0773	H16	0.1308
C5	−0.1039	H17	0.1308
C6	−0.1039	H18	0.1311
C7	−0.1184	H19	0.1311
C8	−0.1184	H20	0.1350
C9	−0.1328	H21	0.1350
C10	−0.1328	H22	0.1122
C11	−0.1258	H23	0.1122
C12	−0.1258		

[a] See structure **1** for details. [b] Geometry data are obtained from ref 21.

TABLE II: Partial Atomic Charges for Water and Ammonia Molecules

molecule	atom	partial charge
H_2O	O	−0.3827
	H	0.1914
NH_3	N	−0.3957
	H	0.1319

Experimental Procedure

The supersonic jet apparatus has been described in detail previously.[10] For time-of-flight mass spectroscopy, the doubled output of two pulsed dye lasers, each of which is pumped by the doubled output of a Nd:YAG laser, is used to excite the fluorene molecule and clusters to S_1, and then ionize it. The pump laser ($S_1 \leftarrow S_0$ excitation) is scanned while the ionization laser (ion $\leftarrow S_1$ excitation) is held at a fixed frequency. The energy of the ionization laser is kept lower than that of the pump laser so as to minimize the fragmentation of the clusters. The two laser beams are made collinear and intersect the expansion gas at right angles. The ions produced are accelerated up the flight tube and detected by a microchannel plate. For the dispersed emission (DE) detection system[11] a 1-m McPherson monochromator with a 1200 g/mm grating is used in the third order to resolve the fluorescence. The emitted light is detected by a photomultiplier tube.

Supersonic expansions are created in a vacuum chamber by using a pulsed nozzle with a 0.7 mm diameter orifice, or a CW

---

(1) Flurry, Jr., R. L.; Wilson, K. R. *J. Phys. Chem.* **1967**, *71*, 589.
(2) Donckt, E. V.; Nasielski, J.; Thiry, P. *Chem. Commun.* **1969**, 1289.
(3) Cheshnovsky, O.; Leutwyler, S. *Chem. Phys. Lett.* **1985**, *121*, 1.
(4) Cheshnovsky, O.; Leutwyler, S. *J. Chem. Phys.* **1988**, *88*, 4127.
(5) Cheshnovsky, O.; Leutwyler, S. *Chem. Phys. Lett.* **1988**, *144*, 317.
(6) Solgadi, O.; Jouvet, C.; Tramer, A. *J. Phys. Chem.* **1988**, *92*, 3313.
(7) Nimlos, M. R.; Kelley, D. F.; Bernstein, E. R. *J. Phys. Chem.* **1989**, *93*, 643.
(8) Law, K. S.; Bernstein, E. R. *J. Chem. Phys.* **1985**, *82*, 2856.
(9) Wanna, J.; Menapace, J. A.; Bernstein, E. R. *J. Chem. Phys.* **1986**, *85*, 1795.
(10) Schauer, M.; Bernstein, E. R. *J. Chem. Phys.* **1985**, *82*, 726.
(11) Breen, P. J.; Warren, J. A.; Seeman, J. I.; Bernstein, E. R. *J. Chem. Phys.* **1987**, *87*, 1917.

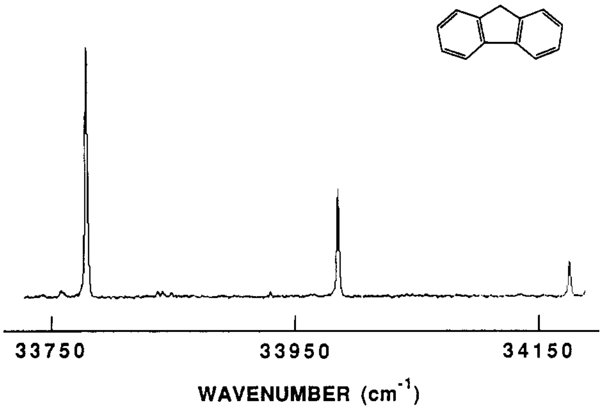

Figure 1. Two-color TOFMS of jet-cooled fluorene. The origin, 0_0^0 transition, for the $S_1 \leftarrow S_0$ transition is at 33778.1 cm^{-1}. The two features +208 and +408 cm^{-1} from the origin are assigned to the totally symmetric vibrations ν_1 and ν_2.

nozzle with a 0.1 mm diameter orifice. Samples of fluorene are placed in the head of the nozzle, enabling the samples to be heated to 70 °C in the pulse nozzle and 150 °C in the CW nozzle.

The expansion gas is typically helium and the backing pressure is about 3–4 atm. Mixtures of helium with NH_3, ND_3, H_2O, D_2O, and piperidine are prepared before they enter the nozzle. The concentration of each solvent is monitored to be 1 or 1.5% in He. Fluorene is purchased from Aldrich and used without additional purification.

The stable geometries of various clusters are calculated by using empirical atom–atom potential energy calculations developed by Scheraga et al.[12] The potential function form is described in detail in a previous publication.[7] The partial charges for each molecule are calculated from the MOPAC (v. 5.0) programs.[13] Table I contains the partial charges of the solute molecule (fluorene), and in Table II the partial charges of the solvent molecules are presented. The atomic numbering of the fluorene molecule is shown in structure **1**.

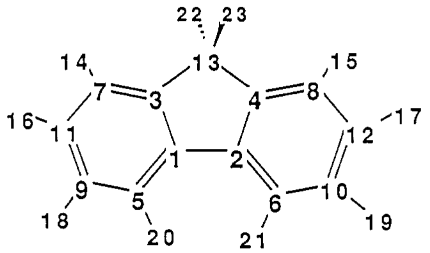

1

Results and Discussion

A. Isolated Fluorene Molecule. The fluorescence excitation and TOFMS of jet-cooled fluorene have been reported previously.[14] The TOFMS of fluorene (m/e = 166) is shown in Figure 1 and is similar to that reported by Leutwyler et al.[14b] The origin is identified at 33778.1 cm^{-1}. The other two intense peaks in the spectrum at +208 and +408 cm^{-1} from the spectral origin are assigned as the totally symmetric 1^1 and 2^1 vibrational modes of S_1, respectively. The assignments are based on those given in ref 14b.

The DE spectrum of jet-cooled isolated fluorene, excited at the origin (33778.1 cm^{-1}), is shown in Figure 2. The two vibrational modes 1_1 and 2_1 in the ground state are identified at 210 and 411 cm^{-1}, respectively.

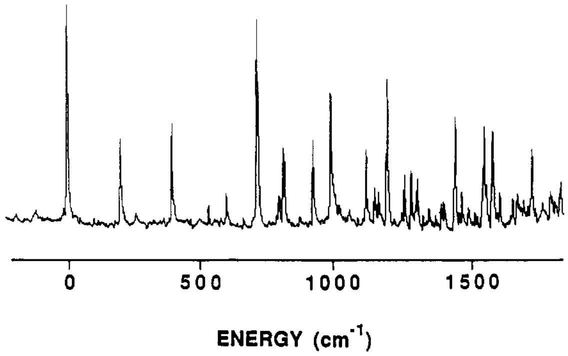

Figure 2. Dispersed emission spectrum of jet-cooled fluorene. The excitation energy is 33778.1 cm^{-1}, corresponding to the origin transition.

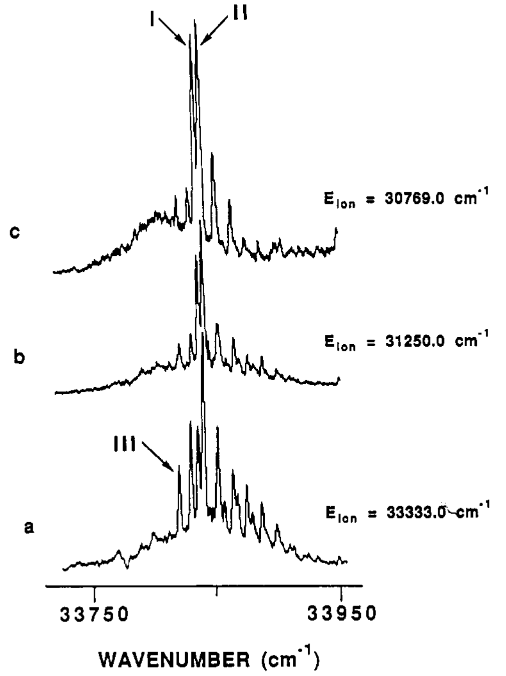

Figure 3. TOFMS of fluorene$(H_2O)_1$ clusters as a function of ionization energy, E_{ion}. (a) E_{ion} = 33333.0 cm^{-1}. (b) E_{ion} = 31250.0 cm^{-1}. (c) E_{ion} = 30769.2 cm^{-1}.

B. Fluorene/Water Clusters. Figure 3 shows the TOFMS of fluorene$(H_2O)_1$ as a function of ionization energy. As ionization energy is decreased, the intensity of two peaks, positioned at 33834.8 (I) and 33840.0 cm^{-1} (II), remains strong. Such an intensity dependence on the ionization energy in the fluorene$(H_2O)_1$ mass channel demonstrates that many of the features attributed to fluorene$(H_2O)_1$ are actually due to fragmentation of larger clusters (mostly the $(H_2O)_2$ cluster), caused by excess vibrational energy in the cluster ion. With the exception of the intense feature at 33840.0 cm^{-1} all the coincident features in the observed $(H_2O)_1$ and $(H_2O)_2$ cluster spectra are probably due to fragmentation of the fluorene$(H_2O)_2$ cluster. Although this latter peak is coincident in energy with a feature in the $(H_2O)_2$ cluster spectrum, its intensity behavior with ionization energy is not indicative of fragmentation of larger clusters.

The DE spectra of the fluorene$(H_2O)_1$ cluster excited at 33834.8 (I) and 33840.0 cm^{-1} (II) and the fluorene$(H_2O)_2$ cluster excited at 33821.3 cm^{-1} (III) are presented in Figure 4. The DE spectrum of fluorene$(H_2O)_1$ excited at 33834.8 cm^{-1} (I) (Figure 4a) evidences two strong peaks in the origin region with a spacing of 51.6 cm^{-1}. Figure 4c presents the DE spectrum of fluorene$(H_2O)_2$ excited at 33821.3 cm^{-1} (III), which shows a vibrational progression with the spacing of 32.4 cm^{-1}. Figure 4b shows three strong peaks in the origin region. The spacing between the origin peak and the next peak in this figure is exactly the same as that in the DE of fluorene$(H_2O)_2$ (32.4 cm^{-1}, Figure 4c) and that between the origin peak and the second peak is exactly the

---

(12) (a) Nemethy, G.; Pottle, M. S.; Scheraga, H. A. *J. Phys. Chem.* **1983**, *87*, 1883. (b) Momany, F. A.; Carruthers, L. M.; McGuire, R. F.; Sheraga, H. A. *J. Phys. Chem.* **1974**, *78*, 1595.

(13) This program is obtained from J. J. P. Stewart and J. A. Menapace at the Frank J. Seiler Research Laboratory, USAFA, Colorado Springs, CO.

(14) (a) Even, U.; Jortner, J. *J. Chem. Phys.* **1983**, *78*, 3445. (b) Leutwyler, S.; Even, U.; Jortner, J. *J. Chem. Phys.* **1983**, *79*, 5769. (c) Amirav, A.; Even, U.; Jortner, J. *Chem. Phys.* **1982**, *67*, 1.

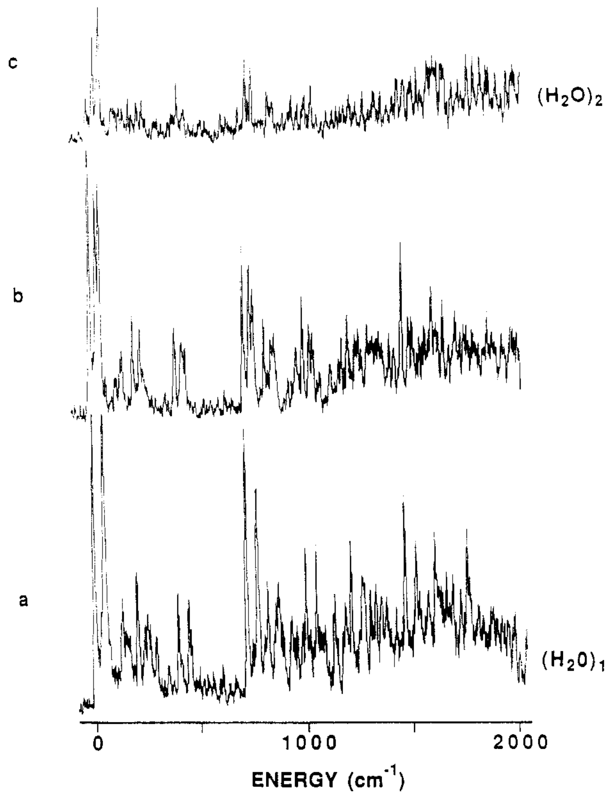

Figure 4. Dispersed emission spectra of fluorene$(H_2O)_n$ ($n = 1, 2$) clusters; (a) excitation at 33 834.8 cm^{-1}, the feature marked I in Figure 3; the transition pumped is assigned to the fluorene$(H_2O)_1$ cluster exclusively; (b) excitation at 33 840.3 cm^{-1}, the feature marked II in Figure 3; the transition pumped is assigned as coincident fluorene$(H_2O)_1$ and $(H_2O)_2$ cluster transitions; (c) excitation at 33 821.3 cm^{-1}, the feature marked III in Figure 3; the transition pumped is assigned exclusively to the fluorene$(H_2O)_2$ cluster.

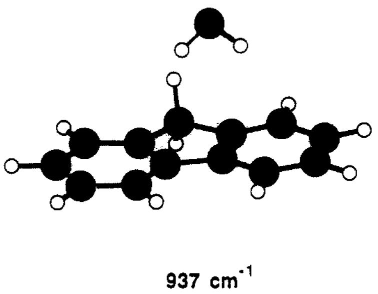

Figure 5. Minimum-energy configuration and binding energy for fluorene$(H_2O)_1$ obtained using a LJ potential calculation.

same as that in the DE of fluorene$(H_2O)_1$ (51.6 cm^{-1}, Figure 4a).

The above DE behavior supports the following conclusions: the peak at 33 834.8 cm^{-1} (I) is only generated by the fluorene$(H_2O)_1$ cluster; the peak at 33 840.0 cm^{-1} (II) is generated by both the fluorene$(H_2O)_{1,2}$ clusters; the second peak (II) in the TOFMS of fluorene$(H_2O)_1$ is due to a vdW vibrational mode since the DE spectra excited at both positions I and II (Figure 3) evidence the same spacing; and only one origin (at 33 834.8 cm^{-1}) is observed for fluorene$(H_2O)_1$.

Only one stable configuration of fluorene$(H_2O)_1$ (binding energy = 937 cm^{-1}) is obtained from LJ potential energy calculations. The structure of this minimum energy cluster is depicted in Figure 5. The oxygen atom of coordinated water is displaced from the center of mass of the fluorene molecule by 0.66 Å along the X axis and is 3.3 Å above the fluorene ring. The water hydrogen atoms are 2.8 Å above the ring.

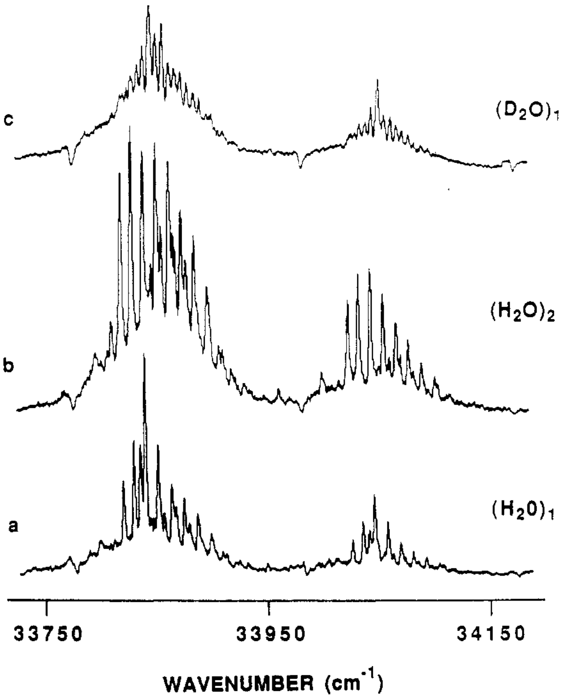

Figure 6. Fluorene/water cluster TOFMS are shown near the origin region for $(H_2O)_1$, $(H_2O)_2$, and $(D_2O)_1$. The TOFMS of fluorene$(H_2O)_1$ and fluorene$(H_2O)_2$ are very similar due to the fragmentation of the disolvate into the monosolvate mass channel (see text). The spacing in the vdW mode progression has decreased by approximately one-half in the fluorene$(D_2O)_1$ spectrum.

TABLE III: Observed vdW Vibrational Energy Levels (cm^{-1}) for S_1 of Fluorene$(H_2O)_2$ and Fluorene$(D_2O)_2$

fluorene-$(H_2O)_2$	fluorene-$(D_2O)_2$	fluorene-$(H_2O)_2$	fluorene-$(D_2O)_2$
0[a]	0[b]	67.07	34.31
9.20	5.72	79.00	39.29
21.13	10.69		44.26
33.00	17.16		49.98
44.69	21.63		55.94
55.63	28.10		62.41

[a] 33 821.3 cm^{-1}. [b] 33 832.9 cm^{-1}.

The two-color TOFMS of fluorene$(H_2O)_2$ clusters and the one-color TOFMS of fluorene$(D_2O)_1$ cluster are presented in Figure 6. The TOFMS of fluorene$(D_2O)_1$ is taken with a high ionization energy (ca. 33 800 cm^{-1}), so that both the mono- and disolvate cluster spectra are present. The fluorene$(H_2O)_2$ cluster spectrum (Figure 6b) shows a progression in a low-frequency mode with a spacing on the order of ~11 cm^{-1}. The spacing of this progession decreases to ~6 cm^{-1} upon deuteration of the water molecule (see Table III). This isotope effect clearly demonstrates that the observed progression is associated with motion of the water molecule and the Franck–Condon intensity profile in this spectrum indicates that a large displacement of the water molecule occurs in the excited state relative to the ground state.

The isotope effect (11 cm^{-1} vs 6 cm^{-1}) for this vdW progression suggests that the motion of the active vdW mode could be a free rotation of the water molecule about an axis that bisects the H–O–H angle because the moment of inertia for this rotation changes by a factor of 2 upon water deuteration. Nonetheless, the harmonic behavior of this vdW mode contradicts the free-rotor explanation. At present, one can only conclude that the active vdW mode is related to the motion of hydrogen atoms most likely (but not definitely) on the water molecule.

The spectra for the mono- and dihydrate fluorene complexes are blue-shifted with respect to the isolated fluorene origin by ~57 and ~36 cm^{-1}, respectively. Cluster features for both the mono- and disolvate complexes are also built on the 1^1 vibration 208 cm^{-1} to higher energy. The cluster features built on this vibration are identical with the cluster features built on the origin.

The spectra of fluorene$(H_2O)n$ ($n = 3$–5) are shown in Figure 7. The cluster spectra become increasingly broad as the number of water molecules increases. The position of the maximum

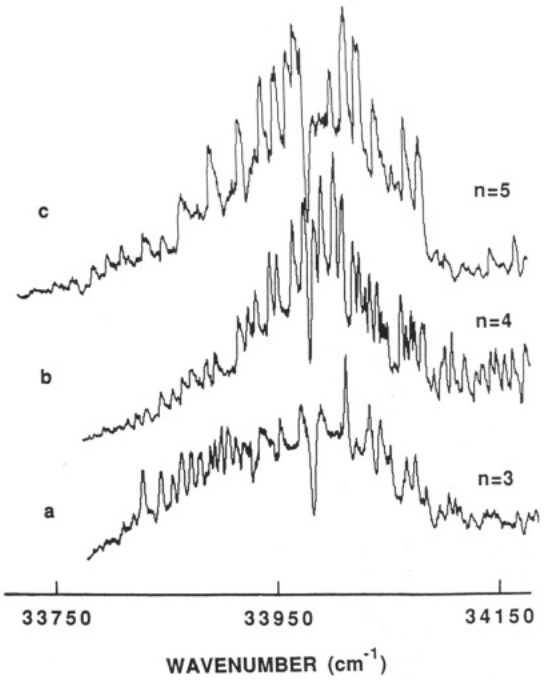

Figure 7. TOFMS of fluorene$(H_2O)_n$ (n = 3–5). The spectra are all broad with sharp features built on the broad background. The negative peak at 33 982 cm^{-1} is due to saturation of the microchannel plate from the ν_1 vibration of isolated fluorene.

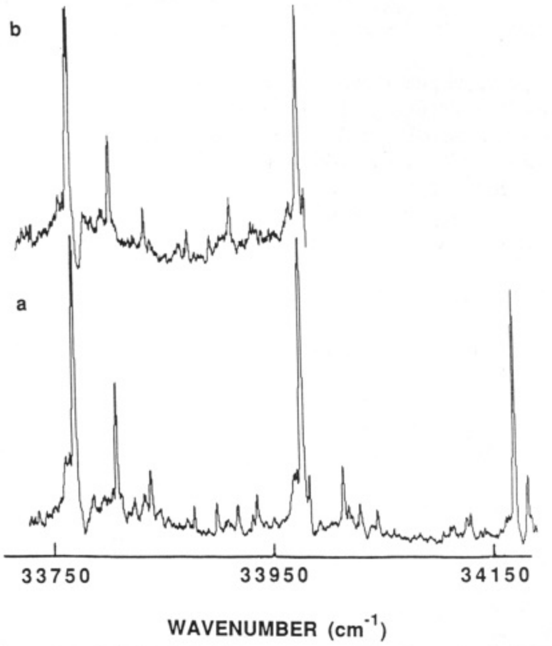

Figure 8. TOFMS of the fluorene(ammonia)$_1$ cluster for both NH_3 and ND_3. The spectra consist of sharp features. In contrast to the results for water clusters, an isotope shift is not observed for the van der Waals modes upon deuteration of ammonia.

spectral intensity (~34 080 cm^{-1}) is almost unchanged as more waters are added to the fluorene$(H_2O)_n$ cluster: such behavior is typical of larger clusters.[15] The increased broadening of the spectra with cluster size can be attributed to several factors: spectral congestion due to multiple cluster configurations, fragmentation of clusters, and/or proton transfer from fluorene to $(H_2O)_n$.

The DE spectra of fluorene$(H_2O)_n$ clusters (n = 3–5) excited at the common maximum-intensity peak, 34 080 cm^{-1} and at ~1000 cm^{-1} excess vibrational energy in S_1 look almost the same as those presented in Figure 4. No highly red-shifted broad emission due to the excited fluorene anion (produced by proton transfer) is observed for this cluster system. Considering the basicity of water and its clusters,[16] this is not a surprising result. The broad and featureless spectra for large fluorene$(H_2O)_n$ clusters must then be attributed to the multiple configurations (and perhaps fragmentation) as n becomes large.

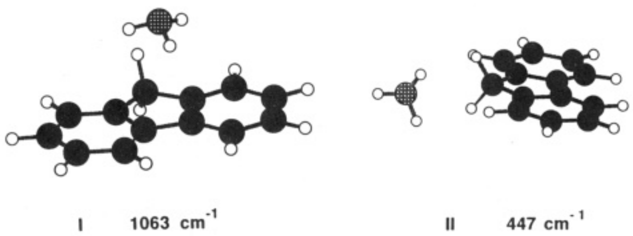

Figure 9. Minimum-energy configurations and binding energies for fluorene$(NH_3)_1$ obtained by using a LJ potential calculation.

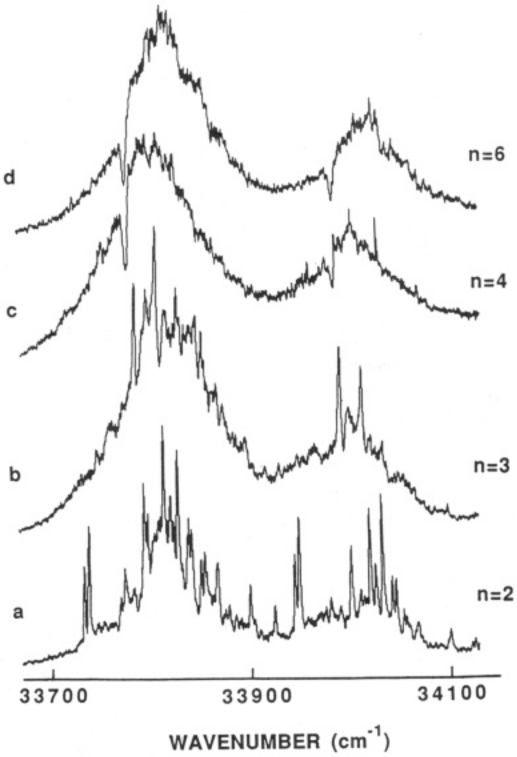

Figure 10. TOFMS of fluorene$(NH_3)_n$, n = 2–4 and 6. The origin of the TOFMS of fluorene$(NH_3)_2$ (taken as the lowest energy doublet) is red-shifted by 51 cm^{-1} from that of the isolated molecule. The spectrum of the disolvate is quite complex consisting of sharp features built on a broad background. As the number of ammonia molecules increases in the cluster, the number of sharp features in the spectrum diminishes and the spectrum becomes broad and featureless.

C. Fluorene/Ammonia Clusters. The TOFMS of fluorene$(NH_3)_1$ (m/e = 183) is shown in Figure 8a. The spectrum is quite sharp and well resolved. The origin for the cluster is red-shifted by 4 cm^{-1} with respect to that of the isolated molecule. Figure 8b depicts the TOFMS of fluorene$(ND_3)_1$ (m/e = 186). The first few features of the fluorene$(NH_3)_1$ and fluorene$(ND_3)_1$ spectra are nearly identical, showing little or no isotopic shift. One can conclude from this observation that at least the first few features correspond to clusters of different configurations.

LJ potential energy calculations support this expectation. Several different minimum energy conformers are obtained from the calculations; for example, one has a geometry in which the

---

(15) Nowak, R.; Menapace, J. A.; Bernstein, E. R. *J. Chem. Phys.* **1988**, *89*, 1309.

(16) Pine, S. H.; Hendrickson, J. B.; Cram, D. J.; Hammond, A. S. *Organic Chemistry*; McGraw-Hill: New York, 1980; pp 200–202.

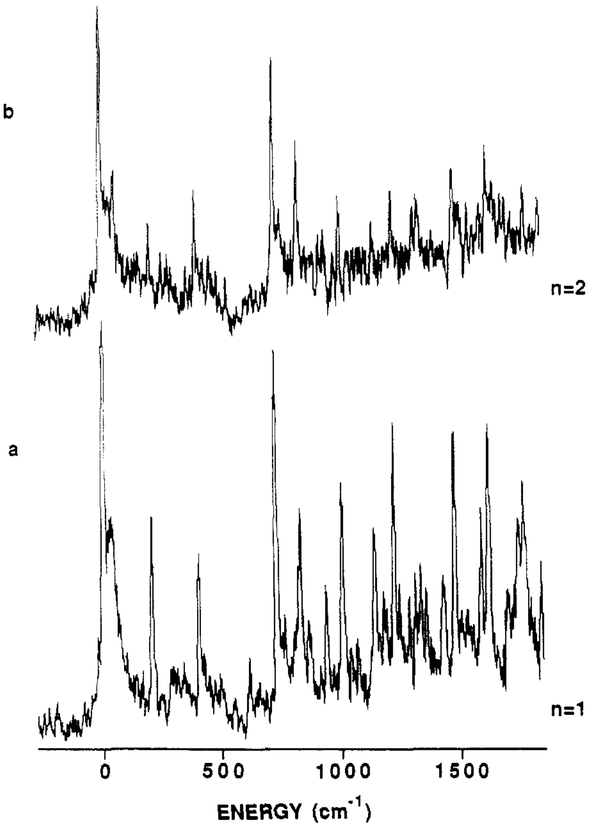

Figure 11. Dispersed emission spectra for fluorene$(NH_3)_1$ and fluorene$(NH_3)_2$. The origin was excited for each of these two clusters, at 33 774.1 and 33 728.6 cm^{-1} for mono- and disolvate, respectively.

ammonia molecule above the fluorene molecule central ring and another has a geometry in which the ammonia molecule coordinates to the aliphatic hydrogens and is displaced from the fluorene ring (see Figure 9).

The TOFMS of fluorene$(NH_3)_2$ is shown in Figure 10a. The origin of this cluster appears as a doublet in the spectrum, red-shifted by 51.3 cm^{-1} with respect to the origin of the isolated molecule. The spectrum of the fluorene$(NH_3)_2$ clusters becomes increasingly more complex at higher energy with several sharp features built on a braod background. The same pattern, both broad and sharp features, is seen to occur in the 1^1 spectra region (~208 cm^{-1} above the origin). The width of this broad peak is on the order of 100 cm^{-1}. The cause of the broadening for this relatively small cluster could be thought to be either dynamical processes or congestion from many possible cluster configurations.

The TOFMS fluorene$(NH_3)_n$ (n = 3–6) are also shown in Figure 10. The spectra are all similar: broad, diffuse, and red-shifted with respect to the isolated molecule. As in the TOFMS of larger fluorene/water clusters, the position of the maximum-intensity peak does not change significantly with fluorene/ammonia cluster size for n = 2–6. The position of this maximum intensity peaak is ~33 810 cm^{-1}.

DE spectra for fluorene$(NH_3)_1$ and fluorene$(NH_3)_2$, obtained by excitation at the cluster 0^0_0, are presented in Figure 11. In both cases (n = 1 and 2), the spectra of the clusters are quite similar to that of the bare molecule with exception of the superimposed vdW cluster structure present in the cluster emission.

A careful search for anion emission (generated by proton transfer from larger fluorene$(NH_3)_n$ ($n \geq 3$) clusters was also performed with excitation energy at 33 810 cm^{-1}. No additional broad fluorescence could be observed in the region 370–550 nm. Moreover, dispersed emission spectra, taken with excess vibrational excitation energy in S_1 of nearly 1500 cm^{-1}, look identical with those presented in Figure 11. These observations suggest that the broadness of the fluorene$(NH_3)_n$ TOFMS is most probably caused by a variety of different cluster conformations for a given cluster mass and not proton transfer/fluorene anion generation.

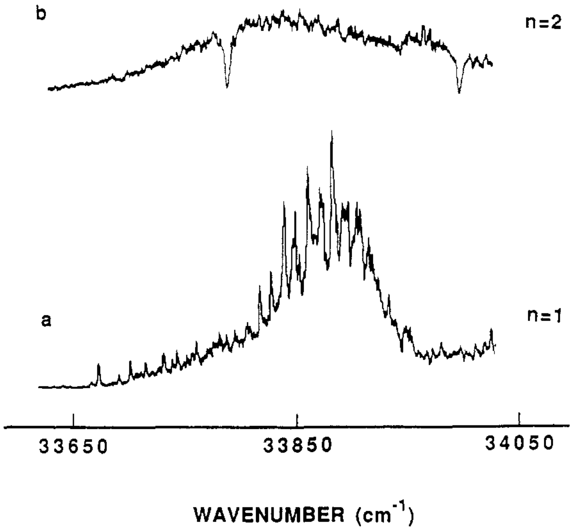

Figure 12. TOFMS of fluorene(piperidine)$_n$ clusters: (a) (piperidine)$_1$; (b) (piperidine)$_2$.

D. Fluorene/Piperidine Clusters. The TOFMS of fluorene/piperidine clusters are present in Figure 12. The spectrum of the monosolvate cluster (Figure 12a) is complex, consisting of both broad and sharp features. The first sharp feature observed in the fluorene(piperidine)$_1$ spectrum is assigned to be the origin of the spectrum. The cluster origin transition is red-shifted by ~90 cm^{-1} compared to the bare fluorene molecule origin. The disolvate spectrum is broad with little or no sharp features (Figure 12b).

DE spectra of piperidine complexes do not show direct evidence for an intermolecular proton-transfer reaction: no broad, red-shifted fluorescence is observed from this system.

E. Proton-Transfer Reaction. Although a Förster cycle calculation of pK_a for the aliphatic hydrogen atoms of fluorene indicates that they are very acidic (pK_a = −8.6) in the excited state and both calculations and experiments suggest that NH_3 and H_2O solvent molecules can coordinate to the aliphatic hydrogens of the fluorene molecule, none of the spectra of these vdW clusters gives any direct evidence for the occurrence of an intermolecular proton-transfer reaction in S_1 (i.e., the generation of the fluorenyl anion). Excited-state proton transfer can only be observed if the proton transfer occurs at least on the same time scale as the lifetime of the excited singlet state S_1 ($\tau(S_1) < 10$ ns). Förster cycle calculations also indicate a large change in pK_a for naphthalene upon excitation (p$K_a(S_0)$ = −4.0, p$K_a(S_1)$ = 11.7);[17,18] however, protonation of naphthalene does not occur upon singlet excitation. Protonation and deprotonation at carbon atoms are apparently quite slow compared to that at oxygen or nitrogen atoms[19,20] and therefore may not be competitive with deactivation of the singlet excited state. Solution-phase studies of proton transfer between the fluorene molecule and methoxy sodium show the rate of this reaction is ~4×10^4 M^{-1} s^{-1};[19] proton transfer occurs in tens of microseconds. A large barrier to proton transfer must therefore exist for this excited-state reaction.

Conclusions

Fluorene$(H_2O)_1$ and -$(NH_3)_1$ vdW clusters show sharp mass-resolved excitation spectra. As the number of solvent molecules is increased ($n \geq 2$) for these clusters, the TOFMS become more complex and broad due to spectral congestion from the many possible stable cluster configurations. In fluorene$(H_2O)_1$,

---

(17) Ireland, J. H.; Wyatt, P. A. H. *Adv. Phys. Chem.*, **1976**, *12*, 131.

(18) Donckt, E. V.; Lietaer, D.; Nasielski, J. *Bull. Soc. Chim. Belg.* **1970**, *79*, 283.

(19) Koch, H. F. *Acc. Chem. Res.* **1984**, *17*, 137.

(20) Kresge, A. J. *Acc. Chem. Res.* **1975**, *8*, 354.

(21) Burns, D. M.; Iball, J. *Proc. R. Soc. London Ser. A*, **1954**, *227*, 200.

only one cluster structure is observed with a (calculated) binding energy of 937 cm^{-1}. In fluorene$(H_2O)_2$, a significant displacement along the vdW coordinates occurs upon $S_1 \leftarrow S_0$ excitation. Studies of fluorene$(NH_3)_n$ and fluorene$(ND_3)_n$ suggest that at least two stable configurations of vdW clusters are possible in fluorene$(NH_3)_1$; one has a structure in which ammonia coordinates to the fluorene ring and the other has a structure in which ammonia is coordinates to the aliphatic hydrogens and is displaced from the fluorene ring.

On the basis of both calculations and interpretation of the fluorene/ammonia, water, and piperidine cluster spectra, one expects that the solvent molecules can coordinate to the aliphatic hydrogens of fluorene molecule in at least some cluster configurations. Nonetheless, no evidence (e.g., broad, red-shifted fluorenyl anion emission) which substantiates an excited-state intermolecular proton-transfer reaction can be found in these systems. The absence of any observed anion emission suggests that the proton-transfer reaction at the carbon center occurs at too slow a rate to be observed given the excited-state lifetime of ca. 10 ns.

Acknowledgment. This work was supported by Office of Naval Research and the National Science Foundation.

Registry No. Fluorene, 86-73-7; ammonia, 7664-41-7; water, 7732-18-5; piperidine, 110-89-4.

Vibrational Structure and Temperature Dependence of the Electronic Absorption ($1^1B_u \leftarrow 1^1A_g$) of *all-trans-β*-Carotene

Hajime Torii and Mitsuo Tasumi*

Department of Chemistry, Faculty of Science, The University of Tokyo, Bunkyo-ku, Tokyo 113, Japan

(Received: June 12, 1989)

The vibrational structure of the absorption spectrum ($1^1B_u \leftarrow 1^1A_g$) of *all-trans-β*-carotene has been analyzed by the second-derivative method and spectral simulation. Estimates of the following quantities have been obtained: the vibrational frequencies and vibrational relaxation rate of the strongly Franck–Condon active modes in the 1^1B_u state, parameters representing the displacement of potential minimum along these modes on going from 1^1A_g to 1^1B_u, and the magnitude of modulation of the 0–0 wavenumber due to intermolecular interactions. Against the primitive inference based on the weakening of bond alternation in the 1^1B_u state, the frequency of the C=C stretch in the 1^1B_u state is higher (though not *greatly*) than that of the corresponding mode in the 1^1A_g state. On the other hand, the frequency of the C–C stretch in the 1^1B_u state is higher by about 90 cm^{-1} than that in the 1^1A_g state, in agreement with the primitive inference. The vibrational relaxation time in the 1^1B_u state is estimated to be of the order of 50 fs. Analysis of the temperature dependence of the absorption spectrum indicates that it is not accompanied by a change in the structure of *all-trans-β*-carotene.

Introduction

all-trans-β-Carotene, a representative polyene having a relatively long chain, is an interesting molecule from spectroscopic and biophysical viewpoints. It has been particularly useful in the studies of second-order optical processes.[1-11] In those studies the Raman excitation profile resonant with the electronic transition $1^1B_u \leftarrow 1^1A_g$ has been analyzed. However, it is surprising to find how scarce is the definite knowledge of the excited state 1^1B_u.

For instance, the vibrational frequencies of the C=C and C–C stretches in the 1^1B_u state are not well determined, although these modes are thought to be strongly Franck–Condon active. By primitive inference, the C=C stretching frequency is expected to become lower to the same extent as the C–C stretching frequency becomes higher on excitation $1^1B_u \leftarrow 1^1A_g$, because of the weakening of bond alternation. On the other hand, in most of the analyses of the Raman excitation profile[1-9] and the absorption spectrum[12] of this molecule, it has been assumed that the frequencies of the two modes in 1^1B_u are the same as those in the ground state 1^1A_g. On this assumption, however, one fails to reproduce the absorption spectrum in the visible region, as shown below (see also Figure 2 of ref 13). This implies that the frequencies become higher (at least on the average) on excitation. For shorter polyenes, this kind of frequency upshift had long been proposed from the absorption or fluorescence excitation spectra at low temperatures,[14-18] and it was clearly observed in the absorption spectra of jet-cooled hexatriene and octatetraene;[19,20] the frequencies of both the C=C and C–C stretches are higher in 1^1B_u than those in 1^1A_g. Furthermore, the parameters used in the analysis of the absorption spectrum and the Raman excitation profile of tetradesmethyl-β-carotene[21] have also indicated the higher frequency shifts. It is therefore expected that *all-trans-β*-carotene (hereafter simply called β-carotene) would be in a similar situation.

Vibrational frequencies of relatively large molecules in excited electronic states are most directly determined by the transient Raman method or the method of fluorescence excitation of jet-

---

(1) Inagaki, F.; Tasumi, M.; Miyazawa, T. *J. Mol. Spectrosc.* **1974**, *50*, 286.

(2) Penner, A. P.; Siebrand, W. *Chem. Phys. Lett.* **1976**, *39*, 11.

(3) Warshel, A.; Dauber, P. *J. Chem. Phys.* **1977**, *66*, 5477.

(4) Sufra, S.; Dellepiane, G.; Masetti, G.; Zerbi, G. *J. Raman Spectrosc.* **1977**, *6*, 267.

(5) Lukashin, A. V.; Frank-Kamenetskii, M. D. *Chem. Phys.* **1978**, *35*, 469.

(6) Siebrand, W.; Zgierski, M. Z. *J. Chem. Phys.* **1979**, *71*, 3561.

(7) Tonks, D. L.; Page, J. B. *Chem. Phys. Lett.* **1979**, *66*, 449.

(8) Hoskins, L. C. *J. Chem. Phys.* **1980**, *72*, 4487.

(9) Ho, Z. Z.; Hanson, R. C.; Lin, S. H. *J. Chem. Phys.* **1982**, *77*, 3414.

(10) Watanabe, J.; Kinoshita, S.; Kushida, T. *J. Chem. Phys.* **1987**, *87*, 4471.

(11) Sue, J.; Mukamel, S. *J. Opt. Soc. Am.* **1988**, *B5*, 1462.

(12) Kjaer, A. M.; Kjaer, N. J.; Ulstrup, J.; Zakaraya, M. G. *Chem. Phys. Lett.* **1989**, *157*, 447.

(13) Okamoto, H.; Saito, S.; Hamaguchi, H.; Tasumi, M.; Eugster, C. H. *J. Raman Spectrosc.* **1984**, *15*, 331.

(14) Gavin, Jr. R. M.; Risemberg, S.; Rice, S. A. *J. Chem. Phys.* **1973**, *58*, 3160.

(15) Granville, M. F.; Kohler, B. E.; Snow, J. B. *J. Chem. Phys.* **1981**, *75*, 3765.

(16) Heimbrook, L. A.; Kenny, J. E.; Kohler, B. E.; Scott, G. W. *J. Chem. Phys.* **1981**, *75*, 4338.

(17) Hemley, R. J.; Dawson, J. I.; Vaida, V. *J. Chem. Phys.* **1983**, *78*, 2915.

(18) Kohler, B. E.; Spiglanin, T. A.; Hemley, R. J.; Karplus, M. *J. Chem. Phys.* **1984**, *80*, 23.

(19) Leopold, D. G.; Vaida, V.; Granville, M. F. *J. Chem. Phys.* **1984**, *81*, 4210.

(20) Leopold, D. G.; Pendley, R. D.; Roebber, J. L.; Hemley, R. J.; Vaida, V. *J. Chem. Phys.* **1984**, *81*, 4218.

(21) Sue, J.; Mukamel, S.; Okamoto, H.; Hamaguchi, H.; Tasumi, M. *Chem. Phys. Lett.* **1987**, *134*, 87. Sue, J.; Mukamel, S. *J. Chem. Phys.* **1988**, *88*, 651.

0022-3654/90/2094-0227$02.50/0